



Luminescence upconversion in GaAs quantum wells

Soheyla Eshlaghi,^{1,*} Wieland Worthoff,¹ A. D. Wieck,^{2,†} and Dieter Suter¹

¹Fakultät Physik, Technische Universität Dortmund, 44221 Dortmund, Germany

²CRHEA-CNRS, rue Bernard Grégory, F-06560 Valbonne Cedex, France

(Received 17 March 2008; revised manuscript received 14 May 2008; published 16 June 2008)

Photoluminescence upconversion removes energy from the medium. It has been applied extensively for laser cooling of atomic vapors and more recently also to condensed matter, such as dye solutions and glasses. The application to semiconductors has also been proposed, but so far, clear evidence is missing. We present a detailed experimental study of photoluminescence upconversion in GaAs quantum wells. We study the conversion efficiency over a wide temperature range as a function of the laser detuning. The best results are obtained when the laser detuning is comparable to the thermal energy, $2k_B T$.

DOI: [10.1103/PhysRevB.77.245317](https://doi.org/10.1103/PhysRevB.77.245317)

PACS number(s): 78.55.-m, 78.40.Fy, 78.67.-n

I. INTRODUCTION

The reduction in the temperature by suitable laser irradiation is a well established technique for cooling free atoms and trapped ions.¹ More recently, similar methods were applied to macroscopic objects with a few degrees of freedom, such as the vibration of a micromirror.^{2,3} Another interesting application would be the reduction in the temperature of condensed matter.^{4,5} Initial demonstration experiments on laser cooling in solids were done by Epstein and co-workers⁶ using rare-earth ions in a glass matrix and shortly afterward by Clark and Rumbles⁷ using a laser dye in a liquid.

Laser cooling works by using thermal energy available in the material to increase the energy of photons: the energy of the emitted photons must be higher than that of the absorbed photons. This process is known as luminescence upconversion or anti-Stokes scattering, depending on the context. Its application to cooling was discussed early in the 20th century⁸ and the corresponding thermodynamics was established by Landau.⁹

In addition to using laser cooling of glasses and liquids, its application to semiconductor materials was also considered.^{4,5} Initial evidence for cooling in semiconductors was presented by Finkeiß *et al.*¹⁰ in 1999, but the interpretation of their results were questioned recently.¹¹

The proposed mechanism for laser cooling in semiconductors is phonon-assisted absorption of photons whose energy is below the band-gap, as shown schematically in Fig. 1. Attempts toward improving the prospects of laser cooling in semiconductors concentrated on the optical efficiency, by eliminating parasitic absorption and improving the coupling efficiency.^{12–14} It was suggested¹² that although the removal of the substrate by lift-off processing increases the nonradiative interface recombination rate, net cooling should be possible for temperatures below 250 K. Improved optical coupling by antireflection coatings and ZnSe hemispheres¹³ should also reduce losses and thereby improve the overall cooling efficiency.

A number of theoretical papers^{15–20} have investigated relevant parameters and suggested possible schemes for improving the cooling process. Relevant parameters for optimization include, apart from the sample quality, the band gap, laser detuning, and pump laser intensity. Loss mechanisms

include carrier trapping leading to nonradiative recombination and photon recycling due to internal reflection.

The main prerequisite for laser cooling is the generation of anti-Stokes photoluminescence (AS-PL). It has been observed in various semiconductor structures at liquid He temperature.^{21–24} However, the anti-Stokes shift observed in these experiments did not arise from phonon-assisted absorption and therefore did not contribute to cooling of the material. Instead, these authors attributed the effect to band bending and surface and dopant effects, to the excitation of biexcitons and Auger processes. Phonon-assisted anti-Stokes photoluminescence (PL) was reported by Finkeiß *et al.*¹⁰ in GaAs/AlGaAs quantum wells (QWs) for temperatures between 40–50 K in different magnetic fields and by Gauck *et al.*¹³ on GaAs/GaInAs heterostructures (GaAs thickness: 0.5–1 μm) at room temperature.

In this paper, we present a detailed experimental study of the AS-PL generated in GaAs quantum wells. We studied the whole temperature range from liquid Helium up to room temperature. The observed PL was from the excitons in single GaAs quantum wells, and we quantified its dependence on detuning of the laser photon energy from the exciton resonance at different temperatures.

The paper is organized as follows: In Sec. II, we describe the sample used for the experiments and its optical properties. Section III gives an overview of anti-Stokes spectra of different quantum wells at different temperatures, and Sec. IV discusses the dependence on the laser detuning. In Sec. V, we show that the best laser cooling efficiency is obtained if

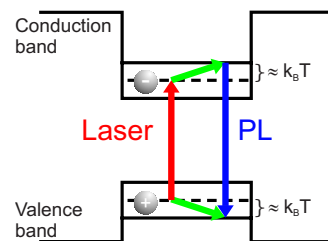


FIG. 1. (Color online) Schematic representation of phonon-assisted photoluminescence upconversion in semiconductor QWs. The full horizontal lines represent the ground state of the corresponding band, the dashed lines intermediate virtual states.

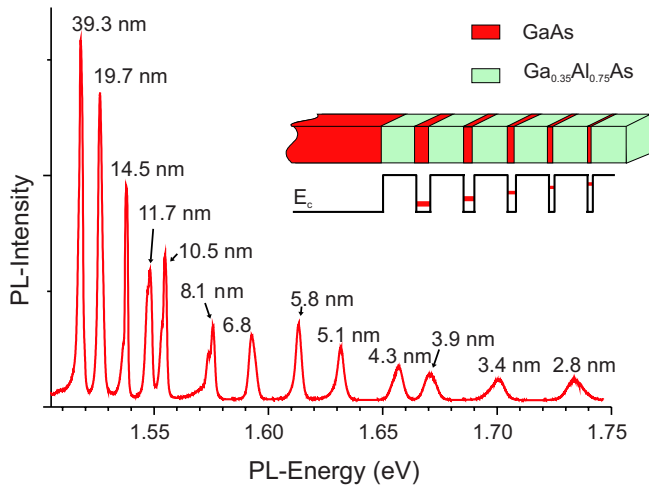


FIG. 2. (Color online) PL Spectrum of the sample at $T=4.3$ K. The sample was excited by a laser diode with a wavelength of 638 nm, corresponding to a photon energy of 1.94 eV. The inset of the figure shows schematically the structure of the sample. The surface is on the right hand side.

the laser is tuned to $\approx 2k_B T$ below the resonance of the exciton. The last section draws a brief conclusion.

II. EXPERIMENT

A. Sample

The sample used in our study was grown by molecular-beam epitaxy on a Te-doped GaAs substrate and consists of 13 undoped GaAs/Al_{0.35}Ga_{0.65}As QWs whose thickness varies from 2.8–39.3 nm. In all measurements, the sample was mounted on the cold finger of a He flow cryostat. The temperature was measured with an AlGaAs sensor mounted close to the sample on the sample holder. An Oxford ITC 502 temperature controller and heater were used to reach temperatures >4 K.

Figure 2 shows the PL spectrum of the sample at 4.3 K when it is excited by a laser diode with a wavelength of 638 nm and an intensity of about 2.5 W/cm². Under these conditions, the excitation photon energy is far above the band gap for all QWs. A schematic representation of its structure is shown in the inset of the figure. The amplitude of the different PL lines is roughly proportional to the thickness of the corresponding QWs.

For all other measurements discussed below, a cw titanium sapphire laser was used, with a tunable wavelength around 800 nm and an intensity of about 50 W/cm². Under these conditions, the photogenerated carrier density is about $N_c \approx 10^{15}$ cm⁻³, if we assume an absorption coefficient of 4×10^4 cm⁻¹ (Ref. 25) and a carrier lifetime of 1 ns (Refs. 26 and 27). The thickness of the QWs decreases from the substrate toward the surface so that the PL from the deeper QWs is not absorbed in the upper layers. The thickness of the Al_{0.35}Ga_{0.65}As barriers is about 31 nm, therefore there is no coupling between different QWs. The photoluminescence was collected by two lenses and passed through a 1 m monochromator (SPEX 1794). A thermoelectrically cooled

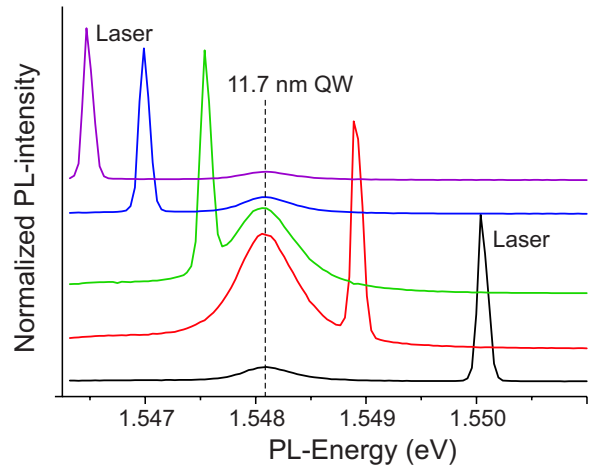


FIG. 3. (Color online) PL spectra of the 11.7 nm QW at $T=14.5$ K (mean PL energy: 1.5482 eV). The laser energy was varied from 1.5465–1.5501 eV.

charged coupled device (CCD) (1024×256 , pixel size 27 μm) was used as detector. The spectral window was about 20 nm so that we were able to detect the PL of several QWs and the scattered light of the laser simultaneously.

In the following, we focus our attention on the 11.7 nm QW. The binding energy of the exciton for this quantum well is about 9 meV.²⁸ For the temperature range studied in the main part of this paper (Sec. IV), the excitonic effects are therefore dominant in the PL spectra ($T < 80$ K, $k_B T < 7$ meV). All measured intensities are normalized (divided by the integrated intensity of the 14.5 nm QW) in order to eliminate the effect of laser power fluctuations.

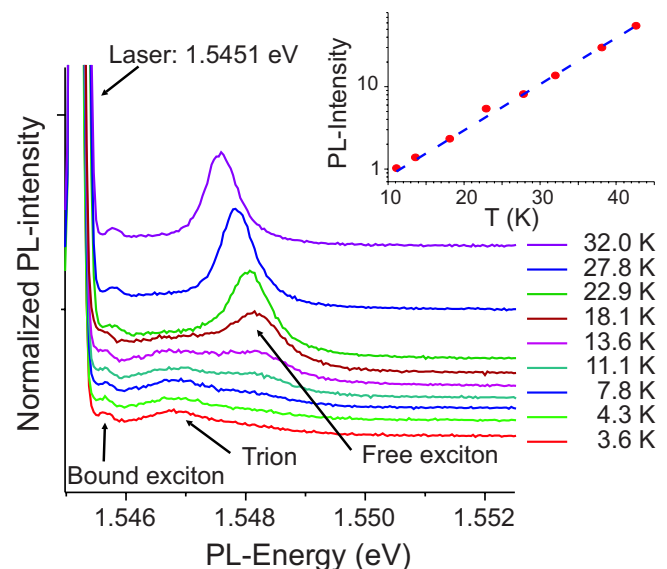


FIG. 4. (Color online) Anti-Stokes PL spectra of the 11.7 nm QW. The PL peaks at 1.5457, 1.5468, and 1.5482 eV correspond to bound excitons, trions, and free excitons. The inset shows the integrated and normalized PL intensities of the free exciton as a function of temperature. An exponential fit of the data indicates a doubling of the PL intensity every 5.3 K.

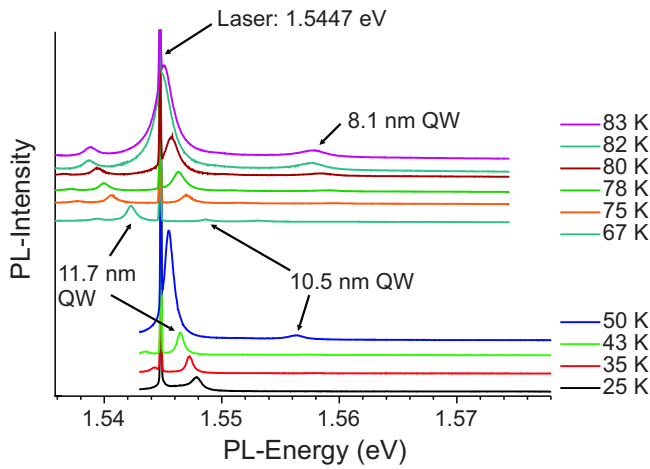


FIG. 5. (Color online) Anti-Stokes PL spectra at various temperatures. New PL lines appear on the anti-Stokes side when the thermal energy exceeds the laser detuning ΔE for the corresponding QWs.

B. Anti-Stokes photoluminescence

The main prerequisite for laser cooling is the observation of anti-Stokes photoluminescence. Figure 3 shows a series of PL spectra, measured at a temperature of 14.5 K. Between the spectra, the laser was set to different wavelengths near the emission wavelength of the 11.7 nm QW.

In each spectrum, the narrow line corresponds to the laser, the broader line, whose position is constant and marked by the dashed vertical line, corresponds to the exciton resonance.

In the three upper spectra, the energy of the laser photons is lower than the exciton energy; in the two lower spectra, the laser frequency is above the resonance. Clearly, the PL signal reaches a maximum when the laser wavelength is close to the resonance line, but the signal from the exciton line remains well observable for a laser detuning of a several meV, for the Stokes—as well as for the anti-Stokes case.

III. TEMPERATURE DEPENDENCE

If the anti-Stokes shift is due to phonon-assisted absorption processes, it should depend on the phonon density and thus on temperature. To verify this assumption, we measured the temperature dependence of the anti-Stokes PL. Figure 4 shows the resulting spectra from the 11.7 nm QW over the temperature range of 3.6–32.0 K.

We first consider the experimental results from the low-temperature region, where the thermal energy of the system is low. For these spectra, we have set the laser frequency to 1.5451 eV, i.e., 3.1 meV below the mean PL energy of the free exciton at $T=4.3$ K.

The PL peaks visible at 1.5457, 1.5468, and 1.5482 eV can be attributed to bound excitons, trions, and free excitons, respectively. At the lowest temperature ($T=3.6$ K), the main signals are due to bound and charged excitons, which are closer to the laser frequency (but still on the anti-Stokes side). For the free exciton, the signal is very small at this low temperature, indicating that the thermal energy is too small

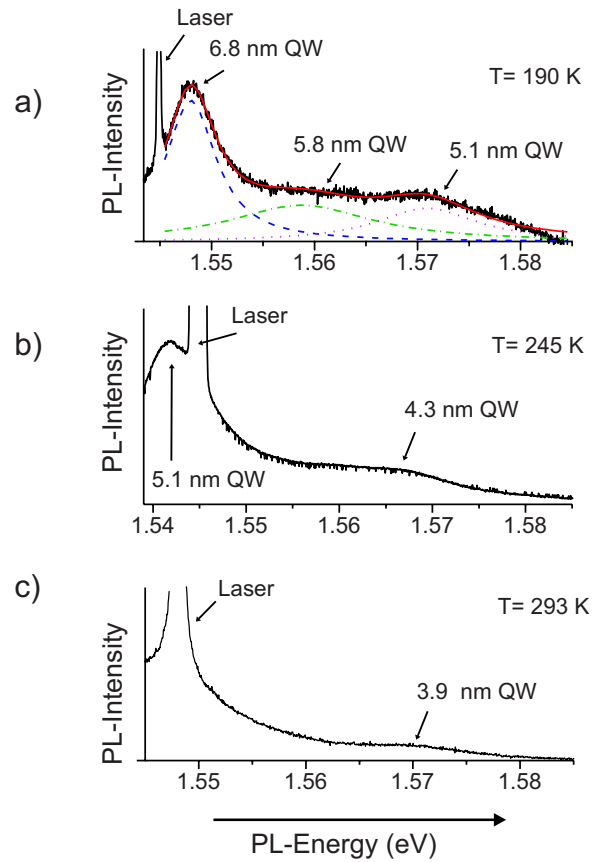


FIG. 6. (Color online) AS-PL of various QWs from 180–293 K. Due to line broadening at these temperatures the PL of different QWs overlaps. At $T=190$ K, we also show a decomposition of the PL spectrum into contributions from the different QWs (Lorentz fits) as well as their sum (red solid line which is almost indistinguishable from the experimental spectrum).

for a significant excitation. With increasing temperature, the signal from the free exciton line increases, while the trion signal disappears at temperatures higher than about 15 K; this appears to be due to the increase in the radiative lifetime of the charged excitons with temperature.²⁹

The inset of the figure shows the integrated and normalized PL intensities for the free exciton transition as a function of the temperature. An exponential fit of these data indicates that the PL increases at a rate of 7.7 K (or 0.66 meV). We attribute this increase to the increase in the phonon density.

In addition, the exciton resonance moves to lower energy with increasing temperature, as the band gap of the QW decreases.^{30–32} As discussed in Ref. 32, it changes for all QWs by ≈ -0.2 meV/K for $40 < T < 130$ K and by ≈ -0.4 meV/K for $T > 130$ K.

Figure 5 shows the corresponding anti-Stokes part of the PL spectra for higher temperatures up to 83 K. The laser excitation energy is fixed to 1.5447 eV. Again, as the temperature increases, the resonance of the 11.7 nm QW moves closer to the laser energy and its amplitude increases.

At temperatures above 60 K, the 11.7 nm QW resonance line has moved to the Stokes side of the laser line and its amplitude decreases again. This is clearly the typical behav-

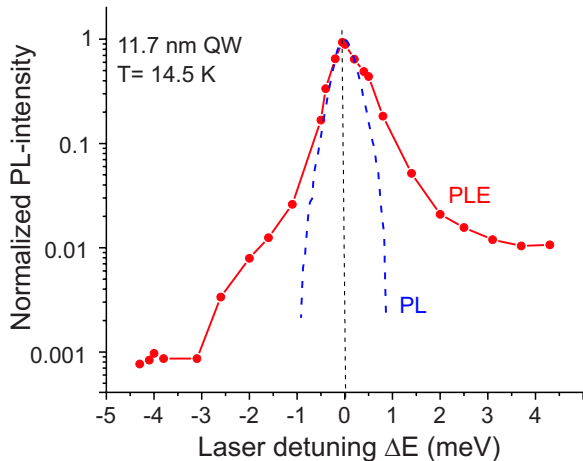


FIG. 7. (Color online) PLE and PL spectra of the 11.7 nm QW at $T=14.5$ K.

ior expected for the offset dependence of a resonant excitation. Exactly the same behavior is observed for the 10.5 nm QW, which first becomes visible at a temperature of 50 K and moves into resonance at 84 K. At temperatures above 80 K, the resonance line of the 8.1 nm QW also becomes visible.

We were able to measure PL upconversion up to room temperature. Figure 6 shows a selection of anti-Stokes PL spectra of different QWs for temperatures from 190–293 K.

At $T=190$ K signal contributions from three QWs with thicknesses of 6.8, 5.8, and 5.1 nm are visible on the anti-Stokes side of the spectrum. In addition a decomposition into contributions from the different QWs (Lorentz fits) is also shown. At these temperatures, the interaction of the excitons with LO phonons causes a significant broadening of the resonance lines, resulting in severe signal overlap. The signal of 5.1 nm QW is anti-Stokes shifted by about 27 meV at 190 K.

With increasing temperature, the line positions shift to lower energy, eventually crossing over to the Stokes side of the spectrum. At the same time, the PL lines of the thinner QWs become visible. At 245 and 293 K the PL of the 4.3 and 3.9 nm QWs are visible, with an anti-Stokes shift of ≈ 22 meV, which shows that luminescence upconversion works at high temperatures even for narrow QWs, even though the absorption cross section is relatively small in these thin films.

IV. DETUNING DEPENDENCE

To get a clearer picture of the relevant processes, we measured the PL as a function of laser detuning at different temperatures. The results depend on temperature and show effects due to phonon density and subband structure of the material.

A. Near-resonant excitation

We examined the near-resonant excitation by scanning the laser over the resonance of the exciton and measuring the integrated PL intensity. Figure 7 compares the photolumines-

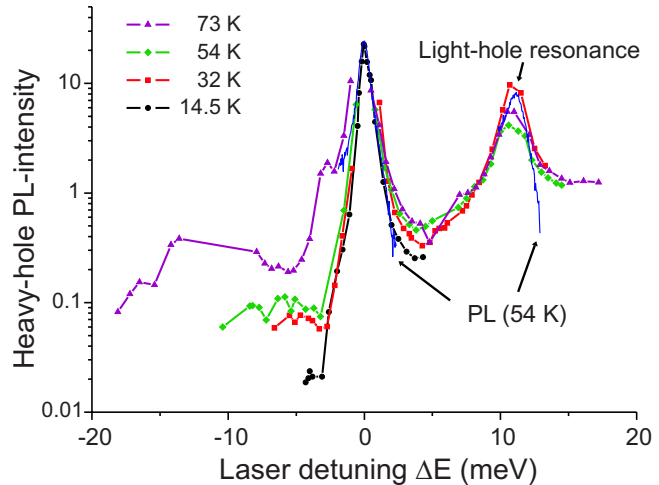


FIG. 8. (Color online) Integrated and normalized hh PL intensity for the 11.7 nm QW at various temperatures as a function of the laser detuning $\Delta E = E_{\text{laser}} - E_{\text{PL}}$.

cence excitation (PLE) and PL spectra for the 11.7 nm QW at $T=14.5$ K. The red data points were obtained by integrating the signal from the heavy-hole resonance in the spectra of Fig. 3 (after subtracting the contribution from the laser line). The dashed blue line shows the PL spectrum, normalized to the same amplitude at zero detuning. The full width of half maximum (FWHM) for the PL line at this temperature is 0.5 meV.

Clearly, the PL intensity reaches a maximum when the laser frequency is set to the exciton resonance. Within a narrow region close to the exciton resonance, we observe a steep decrease in the PL intensity, which is almost symmetric for Stokes vs anti-Stokes irradiation. For detunings smaller than the PL linewidth, the PLE spectrum is almost identical to the PL spectrum, for larger detunings, the PLE data are above the PL data, and the Stokes to anti-Stokes symmetry is broken. For $|\Delta E| > 3$ meV, the PLE signal becomes independent of the laser frequency; the anti-Stokes emission can be measured for detunings up to -4.3 meV, where it decreases again.

B. Variation with temperature

The detuning dependence of the anti-Stokes excitation depends strongly on the temperature. Figure 8 summarizes this dependence for the 11.7 nm QW at different temperatures.

For this experiment, we measured the amplitude of the heavy-hole (hh) resonance as a function of the laser detuning. At higher temperatures, the anti-Stokes PL could be observed for larger detunings. We therefore extended the range of the excitation for positive as well as for negative detunings. When the laser detuning reaches $\approx +10.7$ meV, we observe an increase in the heavy-hole PL, indicating resonant excitation of the light-hole (lh) resonance, with a transfer of light holes to heavy holes.

For small detunings, less than the width of the PL line, the PLE spectrum is independent of temperature (apart from the line broadening observed in the PL spectrum). This indicates

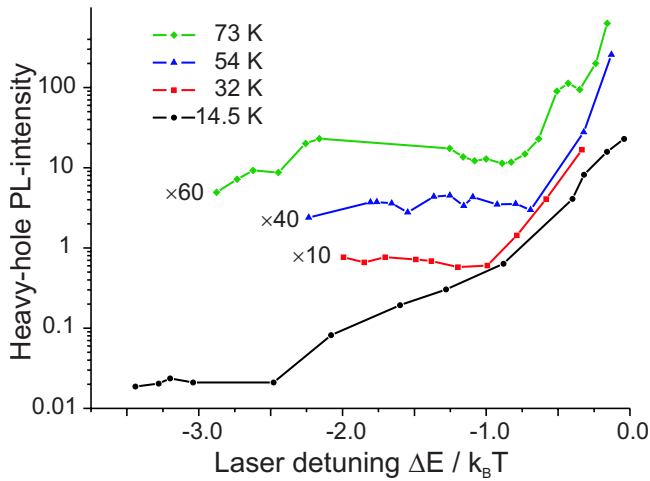


FIG. 9. (Color online) Integrated and normalized intensity of anti-stokes PL as a function of $\Delta E/k_B T$ for the 11.7 nm QW at various temperatures. The data are displaced vertically to avoid overlap.

that in this range, the absorption process does not require assistance by phonons.

If the laser is detuned outside of this region, the PLE spectrum is significantly higher than the PL spectrum. While the temperature dependence of the PLE spectrum is relatively small on the Stokes side, we observe highly significant changes on the anti-Stokes side. While the PLE spectrum decreases more rapidly with detuning on the anti-Stokes side than on the Stokes side, it remains above the PL spectrum throughout by a factor that increases with temperature.

At temperatures above ≈ 50 K, LO phonons are excited and cause significant line broadening at temperatures above ≈ 90 K.³² As a result, the measurements at higher temperatures have a higher detection limit. The corresponding PL linewidths of the 11.7 nm QW are 0.5, 0.6, 0.8, and 1.0 meV at 14.5, 32, 54, and 73 K, respectively.

At 73 K, we have no experimental data between $-13.6 \text{ meV} < \Delta E < -7.9 \text{ meV}$. In this region, the laser excites the heavy-hole resonance of the 14.5 nm QW; this increases the PL of the corresponding light hole, which is very close to the heavy-hole transition of the 11.7 nm QW. As a result, and due to line broadening at the higher temperatures, we cannot reliably measure the PL intensity of the 11.7 nm QW in this range.

The temperature dependence shows clearly that the anti-Stokes PL is excited by thermally activated processes. We therefore compare the PLE spectra by plotting them as a function of the normalized detuning $\Delta E/k_B T$. Figure 9 shows the anti-Stokes part of the PLE spectra from Fig. 8 plotted against the thermally normalized detuning. To avoid overlap, we shifted the spectra vertically by the factors indicated in the figure. At all temperatures, we observe a strong decrease in the PL intensity with increasing detuning, until it reaches a plateau, where it remains roughly constant until the detuning exceeds an energy of about $2k_B T$, where the decrease continues. The height of the plateau, relative to the resonant excitation, is in all cases between 0.01 and 0.03.

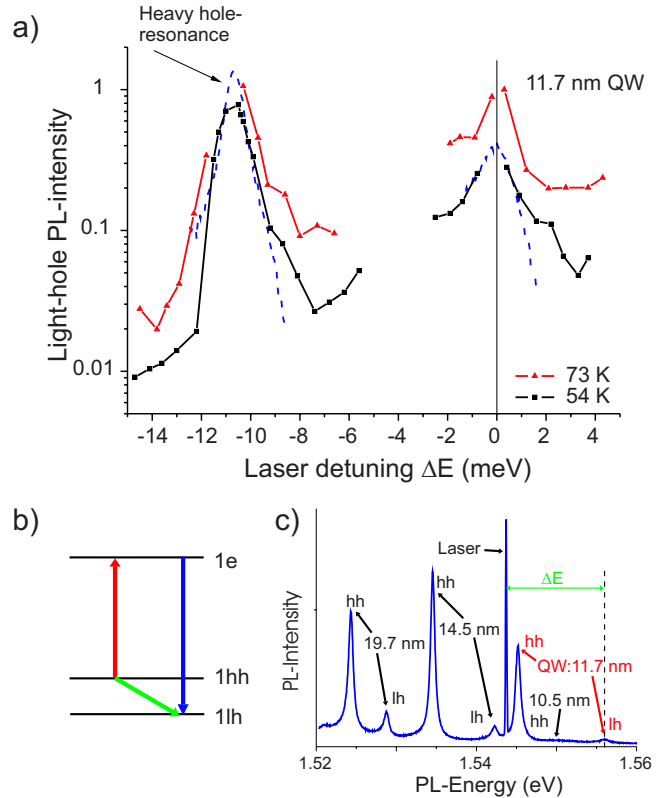


FIG. 10. (Color online) Normalized PL intensity of light hole as a function of laser detuning ΔE at $T=54$ and $T=73$ K for the 11.7 nm QW. The peak at -10.7 meV corresponds to the heavy-hole resonance. The dashed blue lines indicate the corresponding PL spectra at 54 K.

C. Up-conversion to light-hole photoluminescence

So far, we have measured the luminescence of the heavy-hole excitons. As shown in Fig. 8, excitation of the light-hole resonance by the laser also causes a strong increase in the heavy-hole PL, indicating efficient conversion between the different hole types. While this conversion is a simple thermalization, it is also possible to observe the opposite process, i.e., excitation of heavy-hole excitons and observation of light-hole PL, indicating thermally activated upconversion of heavy holes to light holes.

Figure 10(a) shows two PLE spectra of the 11.7 nm QW obtained by measuring the PL at the light-hole resonance and varying the laser excitation energy from -15 to $+5 \text{ meV}$ from the light-hole resonance, at $T=54$ and 73 K . The experimental data clearly show a large anti-Stokes PL at a detuning parameter of $\Delta E = -10.7 \text{ eV}$, which corresponds to resonant excitation of the heavy-hole exciton. The missing data points between -5 and -2 meV are due the resonance of the 10.5 nm QW, which makes it difficult to resolve the light-hole PL of the 11.7 nm QW. Figure 10(b) shows the energy levels of the QW and the relevant processes leading to the anti-Stokes PL and Fig. 10(c) is a representative PL spectrum, where the laser is tuned below the heavy-hole resonance and the light-hole PL is clearly visible $\approx 12.3 \text{ meV}$ above the laser frequency.

The data clearly show that the thermal energy at these temperatures is large enough to convert the heavy holes into

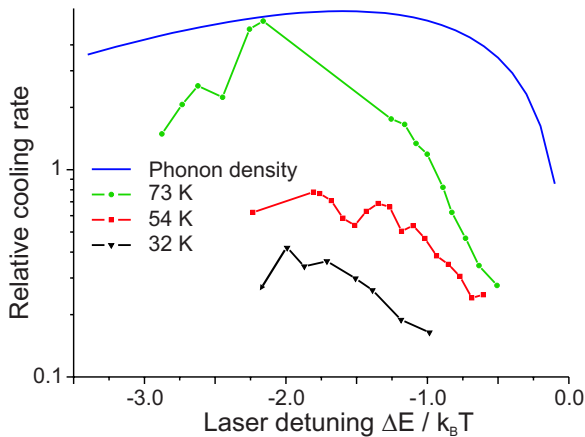


FIG. 11. (Color online) Relative cooling rate (integrated AS-PL multiplied by the detuning $|\Delta E|$) as a function of $\Delta E/k_B T$ for three different temperatures. The blue curve indicates the phonon density as a function of energy.

light holes. This anti-Stokes process is so efficient that the PL of the light hole is actually stronger when the laser excites the heavy hole than when it resonantly excites the light hole.

We observed the same behavior for other QWs and at different temperatures, provided that the thermal energy ($\approx 2k_B T$) of the lattice is sufficiently high to provide the energy difference between the light and heavy holes of the QW. For example, at $T=32$ K we could not measure up-conversion because the thermal energy $2k_B T \approx 5.6$ meV was too low compared to the energy difference between heavy and light hole of 10.7 meV.

V. COOLING RATE

The energy removed from the sample by anti-Stokes PL is equal to the product of the PL intensity and the laser detuning $\Delta E = E_{\text{laser}} - E_{\text{PL}}$. If we evaluate the above data with respect to laser cooling applications, we find that the behavior observed at the different temperatures can be conveniently summarized by calculating the product of the integrated anti-Stokes PL intensity L_{AS} and the anti-Stokes shift ΔE ;

$$\text{Relative cooling rate} = \int I_{\text{PL}}(\nu) \Delta E(\nu) d\nu \approx L_{\text{AS}} \Delta E.$$

The approximation holds for small linewidths, which is well fulfilled in our case, as evidenced by the PL spectra. This

definition corresponds to the radiative recombination term of Sheik-Bahae and Epstein.¹⁷

The measured data corresponding to the above equation are summarized in Fig. 11. While the details differ, we observe in all measurements at $T > 20$ K an increase in the cooling rate with increasing laser detuning $|\Delta E|$, a maximum close to $\Delta E \approx -2k_B T$, and a decrease at larger (absolute) detunings.

The process depicted in Fig. 1 suggests that the anti-Stokes PL should increase with the density of the phonons that provide the energy difference between the photon energy and the energy of the exciton. We therefore compare the experimentally determined cooling rate with the phonon number density dN_{ph}/dE (blue curve in Fig. 11). The curve was calculated as the product of the Bose-Einstein distribution function $\langle n_{\text{ph}} \rangle$ and the (bulk) Debye state density $D(\Delta E) \propto (\Delta E)^2$;

$$\frac{dN_{\text{ph}}}{dE} \propto D(\Delta E) \langle n_{\text{ph}} \rangle \propto \frac{x^2}{e^x - 1}.$$

Here, $x = \Delta E/k_B T$, and we have set the phonon energy equal to the laser detuning ΔE . The comparison between the two sets of curves shows that the maximum of the cooling rate is close to the maximum phonon density at all temperatures.

VI. CONCLUSION

We have presented a comprehensive study of the anti-Stokes PL emission in semiconductor QWs as a function of laser detuning at temperatures from 4 K up to room temperature. We observed a typical resonant behavior close to the exciton resonance, which has the same temperature dependence as the PL line. For larger detunings, thermally activated processes become important. In this range, which extends out to $\Delta E \approx 2.5k_B T$, the absorption cross section is $\approx 2-3$ orders of magnitude lower than at the maximum of the resonance and increases with temperature. The highest cooling rates are obtained for laser detunings of $\Delta E = E_{\text{laser}} - E_{\text{PL}}$ of about $2k_B T$.

In this study, we have only considered the absorption of the laser radiation, not taking into account loss mechanisms or parasitic absorption. Actual applications for laser cooling would have to account for these factors. Since the absorption is highest for thick quantum films, it would be advantageous to use relatively thick layers, possibly multiple quantum films of equal thickness. In addition, it might be necessary to improve the optical coupling efficiency, e.g., by antireflective coatings or hemispheric couplers.¹³

*soheyla.eshlaghi@tu-dortmund.de

†On leave from Lehrstuhl für Angewandte Festkörperphysik, Ruhr-Universität Bochum, 44780 Bochum, Germany

¹S. Chu, *Science* **253**, 861 (1991).

²O. Arcizet, P.-F. Cohadon, T. Briant, M. Pinard, and A. Heidmann, *Nature (London)* **444**, 71 (2006).

³S. Gigan, H. R. Böhm, M. Paternostro, F. Blaser, G. Langer, J. B. Hertzberg, K. C. Schwab, D. Bäuerle, M. Aspelmeyer, and A. Zeilinger, *Nature (London)* **444**, 67 (2006).

⁴M. Sheik-Bahae and R. I. Epstein, *Nat. Photonics* **1**, 693 (2007).

⁵A. Rayner, N. Heckenberg, and H. Rubinsztein-Dunlop, *J. Opt. Soc. Am. B* **20**, 1037 (2003).

- ⁶R. I. Epstein, M. I. Buchwald, B. C. Edwards, T. R. Gosnell, and C. E. Mungan, *Nature (London)* **377**, 500 (1995).
- ⁷J. L. Clark and G. Rumbles, *Phys. Rev. Lett.* **76**, 2037 (1996).
- ⁸P. Pringsheim, *Z. Phys.* **57**, 739 (1929).
- ⁹L. Landau, *J. Phys. (USSR)* **10**, 503 (1946); L. D. Landau, *Collected Papers*, edited by D. Ter Haar (Pergamon, Oxford, 1965), p. 461.
- ¹⁰E. Finkeiß, M. Potemski, P. Wyder, L. Vinò, and G. Weimann, *Appl. Phys. Lett.* **75**, 1258 (1999).
- ¹¹M. P. Hasselbeck, M. Sheik-Bahae, and R. I. Epstein, *Proc. SPIE* **6461**, 646107 (2007).
- ¹²B. Imangholi, M. P. Hasselbeck, M. Sheik-Bahae, R. I. Epstein, and S. Kurz, *Appl. Phys. Lett.* **86**, 081104 (2005).
- ¹³H. Gauck, T. Gfroerer, M. Renn, E. Cornell, and K. Bertness, *Appl. Phys. A: Mater. Sci. Process.* **64**, 143 (1997).
- ¹⁴T. H. Gfroerer, E. A. Cornell, and M. W. Wanlass, *J. Appl. Phys.* **84**, 5360 (1998).
- ¹⁵G. Rupper, N. H. Kwong, and R. Binder, *Phys. Rev. B* **76**, 245203 (2007).
- ¹⁶J. Li, *Phys. Rev. B* **75**, 155315 (2007).
- ¹⁷M. Sheik-Bahae and R. I. Epstein, *Phys. Rev. Lett.* **92**, 247403 (2004).
- ¹⁸T. Apostolova, D. Huang, P. M. Alsing, and D. A. Cardimona, *Phys. Rev. A* **71**, 013810 (2005).
- ¹⁹D. Huang, T. Apostolova, P. M. Alsing, and D. A. Cardimona, *Phys. Rev. B* **72**, 195308 (2005).
- ²⁰D. Huang, T. Apostolova, P. M. Alsing, and D. A. Cardimona, *Phys. Rev. B* **70**, 033203 (2004).
- ²¹J. X. Shen, R. Pittini, and Y. Oka, *Phys. Rev. B* **64**, 195321 (2001).
- ²²T. Kita, T. Nishino, C. Geng, F. Scholz, and H. Schweizer, *J. Lumin.* **87-89**, 269 (2000).
- ²³T. Kita, T. Nishino, C. Geng, F. Scholz, and H. Schweizer, *Phys. Rev. B* **59**, 15358 (1999).
- ²⁴K. Edamatsu, C. Watatani, T. Itoh, S. Shimomura, and S. Hiyamizu, *J. Lumin.* **94-95**, 143 (2001).
- ²⁵*Zahlenwerte und Funktionen aus Naturwissenschaft und Technik: Band 17a Halbleiter*, edited by O. Madelung, M. Schulz, and H. Weiss, Landolt-Börnstein, New Series, Group III (Springer-Verlag, Berlin, 1982).
- ²⁶J. Feldmann, G. Peter, E. O. Göbel, P. Dawson, K. Moore, C. Foxon, and R. J. Elliott, *Phys. Rev. Lett.* **59**, 2337 (1987).
- ²⁷M. Eickhoff, B. Lenzman, G. Flinn, and D. Suter, *Phys. Rev. B* **65**, 125301 (2002).
- ²⁸B. Gerlach, J. Wüsthoff, M. O. Dzero, and M. A. Smondyrev, *Phys. Rev. B* **58**, 10568 (1998).
- ²⁹A. Esser, E. Runge, R. Zimmermann, and W. Langbein, *Phys. Rev. B* **62**, 8232 (2000).
- ³⁰Y. P. Varshni, *Physica (Amsterdam)* **34**, 149 (1967).
- ³¹M. Grassi Alessi, F. Fragano, A. Patanè, M. Capizzi, E. Runge, and R. Zimmermann, *Phys. Rev. B* **61**, 10985 (2000).
- ³²S. Eshlaghi, Ph.D. thesis, Universität Dortmund, Bochumer University Verlag, 2000.